Raman Spectroscopy Assisted with XRF and Chemical Simulation to Assess the Synergic Impacts of Guardrails and Traffic Pollutants on Urban Soils

Journal:	*Journal of Raman Spectroscopy*
Manuscript ID:	JRS-12-0026.R2
Wiley - Manuscript type:	Research Article
Date Submitted by the Author:	20-Mar-2012
Complete List of Authors:	Carrero, Jose; University of the Basque Country (UPV/EHU), Analytical Chemistry Goienaga, Naiara; University of the Basque Country (UPV/EHU), Analytical Chemistry Olivares, Maitane; University of the Basque Country (UPV/EHU), Analytical Chemistry Martinez-Arkarazo, Irantzu; University of the Basque Country (UPV/EHU), Analytical Chemistry Arana, Gorka; University of the Basque Country (UPV/EHU), Analytical Chemistry Madariaga, Juan; University of the Basque Country (UPV/EHU), Analytical Chemistry
Keywords:	Guardrail, Traffic pollutants, Raman Spectroscopy, Urban soils, Chemical simulation

Raman Spectroscopy Assisted with XRF and Chemical Simulation to Assess the Synergic Impacts of Guardrails and Traffic Pollutants on Urban Soils

Jose Antonio Carrero, Naiara Goienaga, Maitane Olivares, Irantzu Martinez-Arkarazo, Gorka Arana, Juan Manuel Madariaga

Abstract

Urban soils are potential reservoirs of toxic metals as a consequence of traffic emissions. Sources like brake linings, tyres, road pavement, exhaust fumes, guardrail, traffic signals and other galvanized steel structures are used in a large variety of external constructions in the modern urban areas. Their beneficial properties from a corrosion and oxidation perspective are well known, but less is known about their contribution to the environmental fate of corrosion-induced released zinc. In this work the impact of guardrails and other traffic pollutants on urban soils has been studied by means of Raman spectroscopy (molecular speciation) and thermodynamic speciation to understand the mechanisms of metal release and uptake by the soils. Hydrozincite, $Zn_5(CO_3)_2(OH)_6$, was identified by means of Raman spectroscopy as the degradation compound of the galvanized zinc layer from guardrails which leads to the formation of soluble zinc, by acidic attack of the urban atmosphere, that drops and accumulate (zinc nitrate was identified) in soils. This fact shows the environmental risk of zinc release from the guardrails since zinc nitrate can be easily mobilized by water runoff, affecting the surrounding areas or groundwater. Other traffic pollutant that reaches guardrail and soil by atmospheric deposition, such as barium, was also identified in soil as well as in the guardrail in its carbonate form, $BaCO_3$. Due to its low solubility, barium will accumulate in urban soils.

INTRODUCTION

Road traffic is one of the most important environmental problems in many cities and the main source of pollution of urban soils, where high levels of toxic metals have been reported as a consequence of traffic emissions (Pb, Ba, Zn, Cd, Sb and Cu among others)[1-5]. Well-known road traffic related metal emission sources of concern are brake linings, tyres, road pavement and exhaust fumes[6-8]. But also guardrail and traffic signals, which are present along the entire road with thousands of kilometres of galvanized steel, involve a potential risk of zinc pollution for urban soils, since they are made from steel plates with an external galvanized layer of Zn[9].

In atmospheric environments the metals suffer deterioration, due to the spontaneous corrosion process, when their surfaces get wet. Zinc coatings are predominantly used to improve the aqueous corrosion resistance of steel by two methods, barrier protection and galvanic

protection[10,11]. Hot-dipped galvanized coatings are widely used as corrosion protection of steels in a large variety of external constructions in the modern urban society like guardrails, lampposts, traffic signals, facades or roofs. In most atmospheric environments, Zn corrodes much less than steel due to the formation of a protective layer consisting of a mixture of zinc oxide and various basic zinc salts depending on the nature of the environment[9,12,13].

An oxide layer formed in that way can be transformed into a non-protective layer by being removed physically (winds and sand erosion), or by partial dissolution of the newly formed products due to rain wash or water condensation on the metal surface. When part of the metal is dissolved by rain, for example, metal ions fall from the metal surface to the soil surrounding the structure, then percolate through the soil and are transported to the groundwater. This phenomenon is recognized today as a metal runoff process[13-16]. As a consequence of metal runoff certain amounts of different metals (zinc, iron, copper and lead), which are originated from the corroded surface of metal structures or from traffic emission, have been detected in soils and waters, and in the biosphere in countries in the EU and USA.

The analysis of the literature shows that since 1990 in Europe and USA the attention given to the metal runoff is considerable[15,17]. In the particular case of Bilbao (north of Spain), a city with past events of severe pollution due to its high density of heavy industries, the problem of the runoff is starting now to be observed because the environmental measures taken by the authorities since thirty years ago have had a great success[18]. A recent work, has demonstrated the good quality of the sediments in the river crossing the city and show that the historical sources of metal pollution are now under control[19]. The data obtained during this three-year period from the “low metal content” sampling points in sediments from the city centre of Bilbao, suggest that when concentrations are close to those of the background values (mineralogical composition of the basin), a seasonal trend is observed, with higher concentrations in summer and lower concentrations in winter. This increase and decrease cycle can only be explained by the input of metals from non-point sources, like the city runoff, because the point sources are not impacting nowadays.

The traffic impact on urban soil in the Metropolitan area of Bilbao has been studied in previous works[20,21]. High concentrations of several metals were found in these urban soils and could be attributed to traffic emissions. Metals accumulate in topsoil and their concentrations decrease quickly with depth and the distance to the road. A special behaviour for zinc was found. Zinc concentration was higher than other metals just under the guardrail and this anomalous local concentration values could not be attributed only to traffic emissions. Thus, a new study was carried out in order to asses the synergic impacts of the guardrails and traffic pollutants on urban soils and to understand the mechanism of metal release. Soils and guardrails from a highly dense road were selected to perform the work. Metals can be more or less mobile in the soil, in relation to their geochemical form which affects their solubility and thus their

bioavailability[22]. Therefore, metal speciation by molecular spectroscopy techniques is important in order to evaluate metal mobility and potential bioavailability of hazardous compounds[23-25]. The use of Raman spectroscopy provides structural and molecular information about the compounds originated by corrosion of the galvanized steel and gives an idea of the potential risk of the pollutants in soil. These data were complemented with X-Ray fluorescence analysis and thermodynamic speciation models, following a methodology that has been used previously to explain the degradation mechanisms in mural paintings[26], the transformation of copper carbonate compounds in different copper sulphate species by attack of oxalic acid excreted by microorganisms in the presence of calcium sulphate[27] or the impact of different environments on the conservation state of walls and wall paintings in the archaeological site of Pompeii, Italy[28].

EXPERIMENTAL

Samples

The studied area belongs to the Metropolitan Bilbao with a high traffic density and humid and rainy climate. Two guardrails were analyzed in this study, a very old guardrail which has been exposed to the environment during several years and another new one that has been recently placed on the road. The old guardrail is heavily deteriorated showing white areas and having a lot of dust adhered to it (a detailed photograph of this material can be seen in Fig. S1 of the Supplementary Material); black spots were also visible together with dust. The new guardrail has a good appearance; the galvanized layer was in perfect condition with a bright homogeneous grey colour without any spots. Soil at different distances from the guardrail was also investigated: one right under the guardrail and two more soil samples next to it were collected to perform the spectroscopic analysis.

Instrumentation

A portable Renishaw RA100 (Renishaw, UK) microprobe system was used for the Raman spectra acquisition of samples at the micrometric level. The system is equipped with a 785 nm diode laser connected with a fibre optic cable to the measuring probe, a mobile diffraction grating of 1200 lines mm^{-1} and a peltier cooled CCD detector. The laser has a nominal output power of 150 mW at the source and some filters allow working at 1%, 10% or 100% of that power. The micro-probe mounted on a tripod is coupled to a 20X objective and incorporate a micro-TV camera whose positioning is controlled by a X,Y motorised micrometric stage allowing perfect focussing of the different mineral grains or surface particles to be analysed.

Guardrails were analyzed at the laboratory, using a hand-held innoRam Raman spectrometer (BWTEK, Newark, EEUU) provided with a 785 nm excitation laser. The microprobe was used in the laboratory with the 20X long-distance objective.

Elemental measurements directly on the surface of the guardrail and on the soil samples were carried out to complement the molecular results. With this aim a portable ArtTAX μ-ED-XRF (Bruker AG) equipped with an X-ray tube with a molybdenum anode working at a maximum voltage of 50 kV and a maximum current of 0.6 mA was used. The X-rays are collimated by a tantalum collimator with a diameter of 0.65 mm and the beam diameter in the sample's surface is 200 μm^2. A CCD camera integrated in the measuring head gives an image of the sample surface (8mm×8mm) and a motor driven XYZ positioning unit allows focusing on different parts of the sample. Samples were analysed directly without any pre-treatment and the operating conditions were fixed at 1000 s, at a voltage of 50 kV and a current of 0.5 mA.

Pre-treatment of the soil samples for Raman analysis

The clay matrix of the soil gives a great fluorescence phenomenon, which saturates the Raman signal. In addition to this, the presence of organic matter can contribute to enhance the fluorescence phenomena and origin interferences in Raman spectra. Both problems difficult the interpretation of the spectra. Therefore, different pre-treatments were carried out.

On the one hand, short acquisition times at low intensity power were used for spectra acquisition in order to avoid saturation, but even so, high fluorescence was obtained and the resulting spectra were too noisy. Thus, a pre-treatment of the spectra was carried out prior to identification. In most of the cases, correction of the baseline and smoothing was used to a greater or lesser extent. On the other hand, following previous experience of the research group in Raman analysis of samples with high organic matter content[25], soil samples were first pre-treated with acetone in order to eliminate the possible organic matter of the soil. The pre-treatment consists of a solid-liquid extraction of the soil with acetone during 30 minutes in an ultrasonic bath.

The calibration of the Raman spectrometer was carried out daily with the 520 cm^{-1} silicon band. The measurement conditions vary depending on the gathered signal to noise ratio and the obtained fluorescence, but exposure times from 5 to 30 s and 1–10 accumulations at 1% or 10% power were used in most of the cases. Several spectra were recorded in each selected area for the proper identification of the compounds involved with the WIRE (Renishaw, UK) software between 2200 and 200 cm^{-1} (spectral resolution of 1 cm^{-1} and cutoff of the system around 200 cm^{-1}) and processed with Omnic 7.2 (Nicolet, Madison, WI, USA) software. The interpretation of the results was performed by comparing the obtained spectra with standard spectra contained in our home-made Raman database[29] and those collected in the RRUFF database[30].

RESULTS AND DISCUSSION

Raman spectra of the guardrails

In order to asses the impact of steel plate traffic signals on soils, some Raman spectra were acquired from different parts of the guardrail. Raman laser was focused first on clean areas from the new guardrail's surface. No signal was obtained in these spectra as it was expected, since metallic forms of Fe and Zn are not active in Raman spectroscopy.

Raman spectra from the old deteriorated guardrail showed the presence of different compounds. Fig. S1 shows a photo of the old guardrail where one can distinguish the deterioration state of the guardrail, with several different black, brown and white spots. Raman spectra of most of these spots showed the presence of amorphous carbon suggesting a deposit of organic matter. For instance, Fig. S2 shows a Raman spectrum of one of these black spots where a mixture of the calcite and amorphous carbon spectra were identified. However, Raman spectra of white spots match quite well with degradation compounds of the galvanized Zn layer[9,31] and other traffic pollutants. Fig. 1 shows two Raman spectra obtained in the old guardrail that match a basic zinc carbonate standard, namely hydrozincite ($Zn_5(CO_3)_2(OH)_6$). It must be borne in mind the environment to which these traffic signals are exposed, with thousands of vehicles passing and emitting exhaust gases. Thus, with the time and climate conditions, the guardrails and other traffic signals are exposed to strong corroding conditions; in a first stage, the Zn layer undergoes the classical passivation step and transforms to zincite, ZnO (equation 1), which continues reacting at high humidity conditions with the CO_2 from the traffic exhaust and gives smithsonite, $ZnCO_3$, and/or hydrozincite as it is elsewhere described[13,31,32], depending on the relative humidity and CO_2 partial pressure (equations 2-4).

$$Zn + H_2O + \frac{1}{2}O_2 \longrightarrow Zn(OH)_2 \rightleftharpoons ZnO + H_2O \qquad 1$$

$$ZnO + CO_2 \longrightarrow ZnCO_3 \qquad 2$$

$$5\,ZnO + 2\,CO_2 + 3\,H_2O \longrightarrow Zn_5(CO_3)_2(OH)_6 \qquad 3$$

$$5\,Zn(CO_3) + 3\,H_2O \rightleftharpoons Zn_5(CO_3)_2(OH)_6 + 3\,CO_2\uparrow \qquad 4$$

With the aim of identifying the presence of other metals deposited on the surface of the guardrail, XRF analyses were also perform on both guardrail samples. The Fig. 2a, shows a XRF spectrum from the new and clean guardrail, Fe and Zn are the major elements of its composition. The external Zn layer is thin enough to allow X-Ray penetrating into the steel, explaining why the signal for Fe also appears. In the old guardrail (Fig. 2b), nevertheless, X-Ray emission K_α lines from some different elements such as Ca, Ba, Pb or Sr can also be seen. These elements are related to traffic emissions and its presence in the guardrail is due to atmospheric deposition from traffic pollution[20,21].

Regarding the Raman spectrum of the white spots in the old guardrail (Fig. 1), the presence of other carbonates is also possible due to the presence of a broad band at 1060 cm^{-1} that could be the unresolved sum of bands belonging to the symmetric stretching of different carbonate compounds. In this sense, the band observed at 690 cm^{-1} indicates the presence also of witherite, $BaCO_3$ (Ba has been detected by XRF in these white spots). The rest of the bands are assigned to the hydrozincite compound. Bands at 707 cm^{-1} and 735 cm^{-1} are not totally resolved as in the hydrozincite standard obtained from the online RRUFF database[30], and it appears to be a double band. One of the guardrail spectra also shows a band at 272 cm^{-1} that it is not present in the standard of the RRUFF database but it is referenced in the work of Hales[33], where they characterized the Raman spectrum of hydrozincite. That work states that the hydrozincite spectrum could present a shoulder at 1078 cm^{-1}, which matches with the spectra obtained from the guardrail in this work. The feature centred at 1062 cm^{-1}, corresponding to the carbonate, shows another band (a shoulder) at 1075 cm^{-1}.

Some chemical equilibrium models were simulated by means of the MEDUSA program[34]. This program can construct different equilibrium diagrams based on the equilibrium information (possible equilibria and their corresponding constants) listed in an electronic database (HYDRA). The Zn layer covering the steel plate is attacked by the acid (rain and/or aerosol) resulting from the CO_2, NO_x and SO_x acid gases present in the urban atmospheres, especially near the traffic areas. Fig. 3a simulates corrosion conditions of the guardrail. The diagram of species of zinc is represented. Solid zinc, oxygen and CO_2 were considered as components of the system; CO_2 concentration was set to 1.7 mM based on measurements of the rain in surrounding areas. At acidic pH values zinc is dissolved mainly as the Zn^{2+} cation but between pH 6-7 zinc carbonate is formed and at higher pH values, hydrozincite is formed. At basic pH values (pH>10) hydrozincite leads to zinc oxide. This graph confirms the thermodynamically favourable conditions leading to the formation of hydrozincite in the guardrail as the most stable oxidation compound when zinc is exposed to the environmental CO_2. This result is in agreement with results obtained by Raman spectroscopy. The same model was built up for BaO. Once again the formation of barium carbonate starting from barium oxide is possible according to the thermodynamic model (see Fig. 3b).

Raman spectra of the soil samples

Once zinc is in the hydrozincite form, it is mobilizable by acidic attack and can consequently be released into the environment. These oxidized residues are now soluble in slightly acidic conditions (like those given by the acid rain on high density traffic roads) and can reach soils under the guardrail through the rain wash, or can be detached as a solid from the steel plate. A soil matrix is much more complex than the steel plate from the guardrail. The number of different compounds that could be present in a soil is very high. However, their concentrations vary from thousands of µg/g to less than one ng/g. The interpretation of the Raman spectra of soils could be very difficult without a first idea of the concentration range of the different

elements present in the soil. Therefore, a first screening of the soils under the guardrail was carried out by means of ICP-MS[21]. Semi-quantitative ICP-MS analysis from the soils revealed, an elevated concentration of zinc in top soil. The Zn concentration falls down abruptly from 800 µg/g right underneath to near 50 µg/g only a few centimetres far away. This experimental evidence can only be explained by an input of zinc coming from the guardrail.

Once it was known that there was a release of Zn from the guardrail into the soil and its concentration was high enough to be detected, soil was submitted to Raman spectroscopic analysis in order to identify the molecular form of zinc. Some natural components of soil like calcite ($CaCO_3$) (Fig. S2), dolomite ($CaMg(CO_3)_2$) (Fig. S3) and quartz (SiO_2) (Fig. 4a) were found. These are common components of calcareous clay soils, as is the case of soils from the Basque Country.

Barium was detected also in the soil, apart from in the guardrail, again in carbonate form (Fig. 4a). Barium is released to the environment as BaO used in brake materials. This barium oxide was then detected in the guardrail as $BaCO_3$ (witherite) which means that the BaO particles that deposit on the guardrails (and in soils) react with CO_2 to give the carbonate (equation 5) and then reach the soil with the rain (physical displacement, not solubilisation) and/or wind. The simulation of this chemical system in Fig. 5a confirms that the formation of barium carbonate from barium oxide is thermodynamically feasible. The pH measured in soil samples was 7.7-7.8. At this pH value, $BaCO_3$ is the most stable species of Ba. The second one, another solid species, is $BaSO_4$ (it was not detected by Raman analysis of the soils). The fraction of the only mobilizable species, Ba^{2+}, is lower than 20% of total Ba and therefore, due to its low solubility, $BaCO_3$ will accumulate in urban soils. This fact was experimentally assessed by analysing the total concentration of alkali-earth metals. The geochemical order of concentrations Ca > Sr > Ba was not found in urban soils near roads with high-density traffic where the concentration of Ba > Sr[20,21].

$$BaO + CO_2 \longrightarrow BaCO_3 \qquad 5$$

But the most remarkable thing was the presence of $Zn(NO_3)_2$ among those carbonate compounds in soil samples under the guardrail (Fig. 4b). The chemical equilibrium model for zinc in soil was also simulated. Previous ICP-MS analysis from the soils gave a Zn concentration of about 12 mM. Sulphate and carbonate were added to the system as anions, their concentrations being established based on soil matrix estimation from the soluble salt quantified by ionic chromatography. The redox potential was also measured around 200 mV. With all these parameters the diagram of fractions for zinc chemical model indicates that hydrozincite is the predominant form of zinc in calcareous soils (Fig. 5b). At the typical pH values found in soils, hydrozincite is the most feasible form of zinc in soils. However, $Zn(NO_3)_2$ was detected by Raman spectroscopy (Fig 4b). This fact could be explained by new reactions

undergone by hydrozincite in the soil. Hydrozincite can be dissolved in top soil by the acid gases from traffic exhausts (and/or CO_2) and the soluble Zn^{2+} can react with the nitrate present in soil (or even with the NO_x from traffic exhaust), yielding the more easily mobilizable form of zinc, $Zn(NO_3)_2$ when the soil is dried and the CO_2 is evaporated (equation 6). This fact shows the environmental risk of zinc release from the guardrails since zinc nitrate can be easily mobilized by water runoff and can pollute surrounding areas or groundwater.

$$Zn_5(CO_3)_2(OH)_6 + 10HNO_3 \longrightarrow 5Zn^{2+} + 10NO_3^- + 8H_2O + 2CO_2(g)\uparrow \quad (6)$$

CONCLUSIONS

The aim of this work was to assess the synergic impacts of guardrails and traffic related pollutants on urban soils. The identification of degradation compounds of the galvanized guardrail from roads and highways was performed using Raman spectroscopy and thermodynamic speciation models. Hydrozincite ($Zn_5(CO_3)_2(OH)_6$) was the main patina component on guardrails exposed at nonsheltered conditions for long periods of time. Guardrails were demonstrated to be an important zinc release source to urban soil. Zinc from the galvanized layer of the guardrails oxidized to hydrozincite which can reach the soil when a part of the metal oxide is dissolved by rain. This is a local phenomenon but represents an important environmental risk since zinc nitrate was detected in soil samples and it is easily mobilized by water runoff, polluting surrounding soil and/or water, and reaching sediments of nearby rivers, like it has been observed recently in sediments from the city centre of Bilbao.

Furthermore, barium carbonate could be also detected both in the soil and in the guardrail. BaO particles coming from brake wear deposit on the guardrails (and on soils) and react with CO_2 to give the carbonate. Due to its low solubility this metal is favoured to be accumulated in soils on the roadsides with high traffic density.

Finally, the results obtained highlight the importance of the use of molecular spectroscopy techniques like Raman spectroscopy to detect the molecular species found on the guardrail and the soil, which is fundamental in order to be able to explain the reaction path leading to their formation. Moreover, these results illustrate that the knowledge of total concentration of metals in soil can be important but that it is much more interesting to know is the chemical form in which the metal is found. Thus the question of whether or not the metal is bioavailable in a certain chemical form can be answered so as to assess the risk of its presence.

Acknowledgments

This work has been financially supported by the Spanish Ministry of Science and Innovation through the IMDICOGU project (ref.:BIA2008-06592). J.A. Carrero and N. Goienaga are grateful to the University of the Basque Country (UPV-EHU) for their pre-doctoral fellowships. The

authors are grateful for technical and human support provided by the Raman-LASPEA Laboratory of the SGIker (UPV/EHU, MICINN, GV/EJ, ERDF and ESF).

References

[1] D. S. T. Hjortenkrans, B. G. Bergback, A. V. Haggerud, *Environ. Sci. Technol.* **2007**; *41*, 5224.

[2] K. Adachi, Y. Tainosho, *Environ. Int.* **2004**; *30*, 1009.

[3] E. R. McKenzie, J. E. Money, P. G. Green, T. M. Young, *Sci. Total Environ.* **2009**; *407*, 5855.

[4] E. Apeagyei, M. S. Bank, J. D. Spengler, *Atmos. Environ.* **2011**; *45*, 2310.

[5] X. Chen, X. Xia, Y. Zhao, P. Zhang, *J. Hazard. Mater.* **2010**; *181*, 640.

[6] A. Thorpe, R. M. Harrison, *Sci. Total Environ.* **2008**; *400*, 270.

[7] M. Abu-Allaban, J. A. Gillies, A. W. Gertler, R. Clayton, D. Proffitt, *Atmos. Environ.* **2003**; *37*, 5283.

[8] J. Sternbeck, A. Sjodin, K. Andreasson, *Atmos. Environ.* **2002**; *36*, 4735.

[9] D. Lindström, I. Odnevall Wallinder, *Environ. Monit. Assess.* **2010**; *173*, 139.

[10] X. G. Zhang, *Corrosion and Electrochemistry of Zinc*, Plenum Press, New York, **1996**.

[11] H. Asgari, M. R. Toroghinejad, M. A. Golozar, *Appl. Surf. Sci.* **2007**; *253*, 6769.

[12] I. Odnevall, C. Leygraf, *Corros. Sci.* **1994**; *36*, 1077.

[13] B. Zhang, H.-B. Zhou, E.-H. Han, W. Ke, *Electrochim. Acta* **2009**; *54*, 6598.

[14] L. Veleva, E. Meraz, M. Acosta, *Mater. Corros.* **2007**; *58*, 348.

[15] L. Veleva, E. Meraz, M. Acosta, *Corros. Eng., Sci. Technol.* **2010**; *45*, 76.

[16] M. Mouanga, P. Berçot, J. Y. Rauch, *Corros. Sci.* **2010**; *52*, 3984.

[17] M. E. Tuccillo, *Sci. Total Environ.* **2006**; *355*, 288.

[18] S. Fdez-Ortiz de Vallejuelo, G. Arana, A. de Diego, J. M. Madariaga, *Chemosphere* **2011**; *85*, 1347.

[19] S. Fdez-Ortiz de Vallejuelo, G. Arana, A. de Diego, J. M. Madariaga, *J. Hazard. Mater.* **2010**; *181*, 565.

[20] J. A. Carrero, I. Arrizabalaga, N. Goienaga, G. Arana, J. M. Madariaga, in *Urban Environment*, (Eds: S. Rauch, G. M. Morrison), Springer, Dordrecht, **2012**, pp. 383.

[21] J. A. Carrero, N. Goienaga, O. Barrutia, U. Artetxe, G. Arana, A. Hernandez, J. M. Becerril, J. M. Madariaga, in *Highway and Urban Environment*, (Eds: S. Rauch, G. M. Morrison, A. Monzon), Springer, Dordrecht, **2010**, pp. 329.

[22] A. Kabata-Pendias, H. Pendias, *Trace elements in soils and plants*, CRC Press, New York, **2001**.

[23] N. Goienaga, N. Arrieta, J. A. Carrero, M. Olivares, A. Sarmiento, I. Martinez-Arkarazo, L. A. Fernández, J. M. Madariaga, *Spectrochim. Acta, Part A* **2011**; *80*, 66.

[24] R. L. Frost, T. Kloprogge, M. L. Weier, W. N. Martens, Z. Ding, H. G. H. Edwards, *Spectrochim. Acta, Part A* **2003**; *59*, 2241.

[25] U. Villanueva, J. C. Raposo, K. Castro, A. de Diego, G. Arana, J. M. Madariaga, *J. Raman Spectrosc.* **2008**; *39*, 1195.

[26] M. Perez-Alonso, K. Castro, J. M. Madariaga, *Anal. Chim. Acta* **2006**; *571*, 121.

[27] K. Castro, A. Sarmiento, I. Martinez-Arkarazo, J. M. Madariaga, L. A. Fernandez, *Anal. Chem.* **2008**; *80*, 4103.

[28] M. Maguregui, U. Knuutinen, K. Castro, J. M. Madariaga, *J. Raman Spectrosc.* **2010**; *41*, 1110.

[29] K. Castro, M. Perez-Alonso, M. D. Rodriguez-Laso, L. A. Fernandez, J. M. Madariaga, *Anal. Bioanal. Chem.* **2005**; *382*, 248.

[30] *RRuff Project. Raman spectra database*, http://rruff.info/hydrozincite/display=default/ Retrieved in 12-01-2012.

[31] P. Colomban, S. Cherifi, G. Despert, *J. Raman Spectrosc.* **2008**; *39*, 881.

[32] J. G. Castaño, C. A. Botero, S. Peñaranda, *Rev. Metal Madrid* **2007**; *43*, 133.

[33] M. C. Hales, R. L. Frost, *Polyhedron* **2007**; *26*, 4955.

[34] I. Puigdomenech, *Make Equilibrium Diagram Using Sophisticated Algorithms (MEDUSA)*, Inorganic Chemistry Royal Institute of Technology (KTH), Stockholm, Sweden, **2010,** **http://www.kemi.kth.se/medusa**.

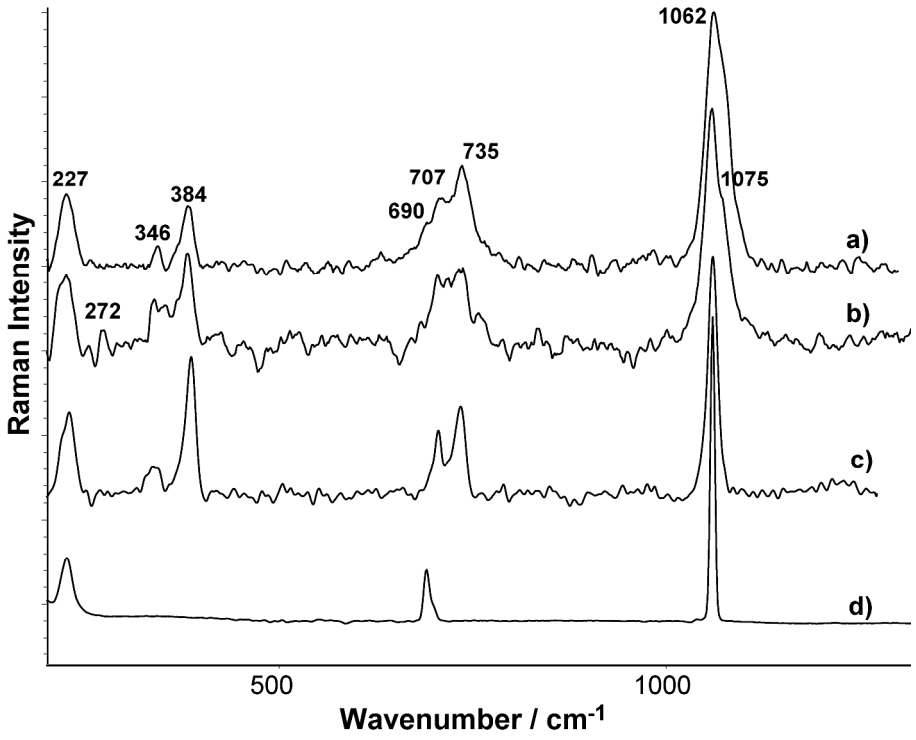

Figure 1. Raman spectra of a) and b) white spots in the old guardrail, c) hydrozincite standard, and d) barium carbonate standard.
387x293mm (300 x 300 DPI)

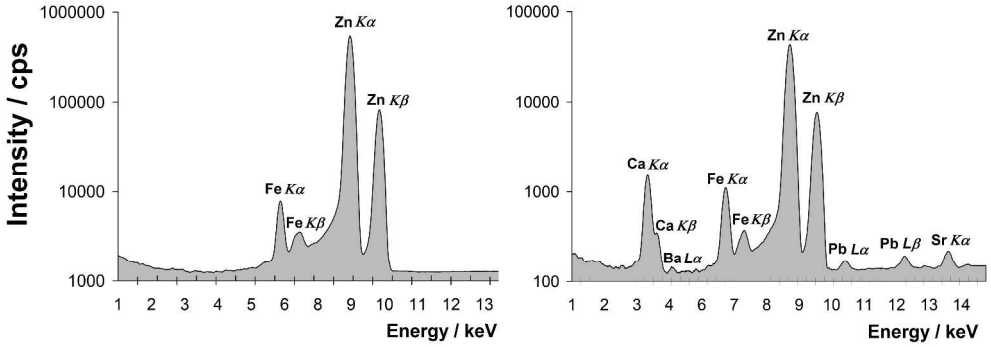

Figure 2. XRF spectra of the a) new guardrail and b) old guardrail.
763x269mm (300 x 300 DPI)

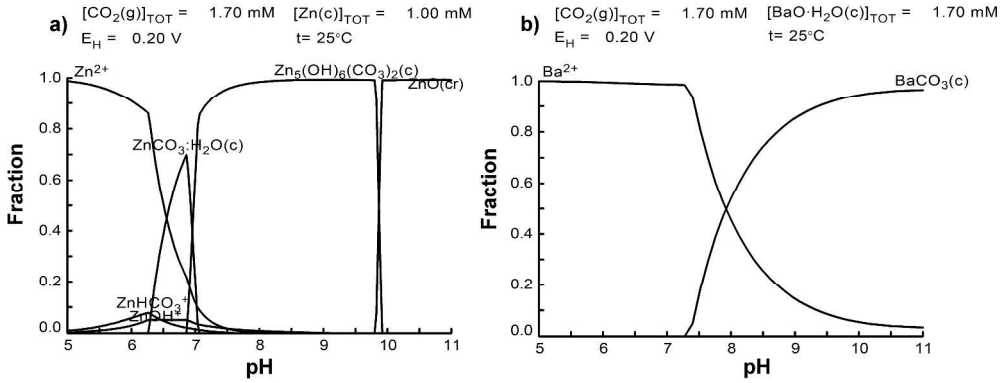

Figure 3. Chemical simulation of the processes given in the guardrail leading to a) hydrozincite and b) barium carbonate.
484x181mm (300 x 300 DPI)

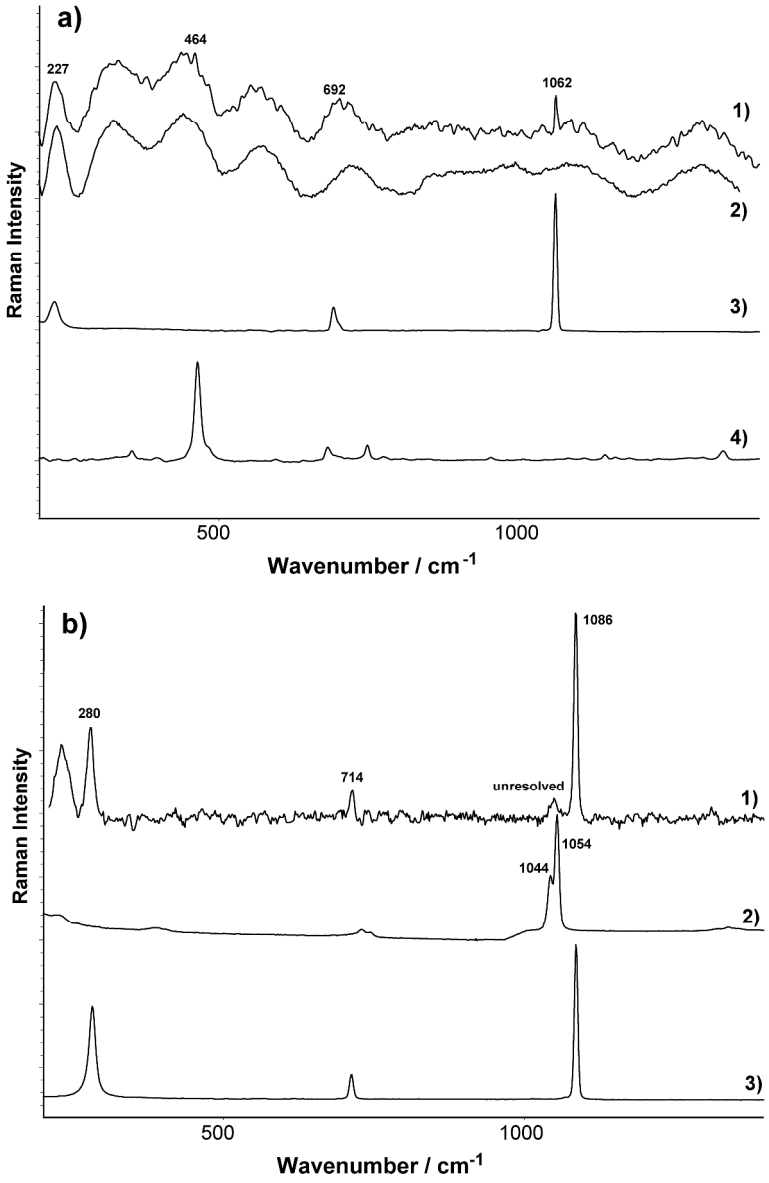

Figure 4. Raman spectra of a): 1) quartz and $BaCO_3$ in soil sample, 2) soil background, 3) and 4) $BaCO_3$ and quartz standards, respectively; and b): 1) $CaCO_3$ and $Zn(NO_3)_2$ in soil sample, 2) and 3) $CaCO_3$ and $Zn(NO_3)_2$ standards, respectively.
387x598mm (300 x 300 DPI)

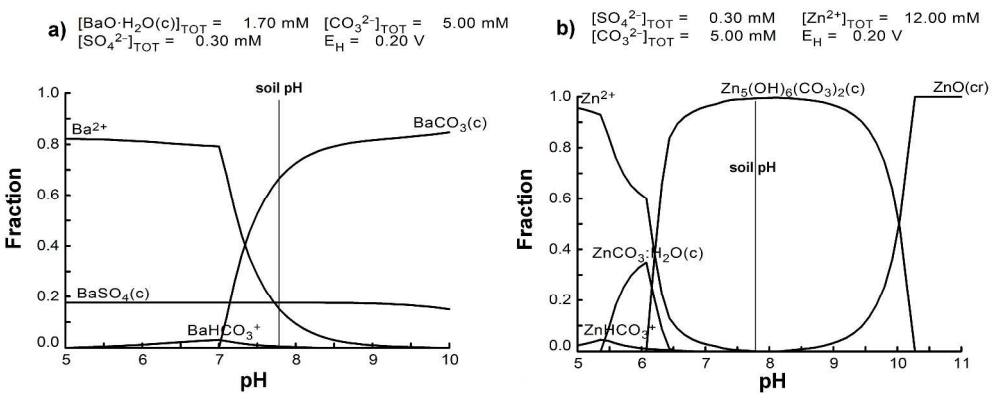

Figure 5. Chemical simulation of barium (a) and zinc (b) compounds in soil.
484x188mm (300 x 300 DPI)